

# Simplified sol–gel method for synthesis of mesoporous alumina

Mahesh P. More, Pravin O. Patil, Abhijeet P. Pandey, Dilip A. Patil, Prashant K. Deshmukh

Department of Pharmaceutics, H R Patel Institute of Pharmaceutical Education and Research, Shirpur,  
Maharashtra 425 405, India  
E-mail: pkdesh@rediffmail.com

Published in Micro & Nano Letters; Received on 12th September 2013; Revised on 24th October 2013; Accepted on 1st November 2013

In the present investigation, a simplified method for the synthesis of mesoporous alumina using a sol–gel strategy is reported. Formation of the mesoporous structure is supported by the results of a Brunauer-Emmett-Teller study. The Fourier transform infrared spectroscopy spectra confirmed its primary characteristic peaks. Elemental analysis and X-ray diffraction revealed the formation of  $\gamma$ -Al<sub>2</sub>O<sub>3</sub>, after calcination at 700°C. Particle size and zeta potential were measured to assess the size and the surface charge of the synthesised mesoporous material.

**1. Introduction:** Emerging research interest has been devoted to the field of mesoporous inorganic nanoparticle synthesis. Inorganic nanoparticles can be defined as particles of metal oxide or metallic composition possessing at least one length scale in the nanometre range. The mesoporous structure offers increased surface area as a result of its intricate and structured network of pores [1].

The preparation of mesoporous alumina (MpAl) with high surface area, a uniform pore structure and narrow pore size distribution is of great interest for both technological applications as well as fundamental research [2]. The synthesis of MpAl (pore size 20 Å) using an alkyl carboxylate as a surfactant and hexagonally mesostructured alumina using dodecyl sulphate and aluminium nitrate have been reported previously [3, 4]. Moreover, MpAl from electrically neutral assemblies of poly(ethylene oxide) and aluminium alkoxides, has also been reported elsewhere [5].

MpAl is superior to mesoporous silica (MpSi) because of its high hydrolytic stability along with a different point of zero charge, which makes it a suitable platform for loading different metal species. The performance of the conventional MpAl, however, is limited because of its uncontrolled porosity and deactivation by choking and plugging that hinders the diffusion of reactants and products [6]. The MpAl has been used as ceramics [7] and catalyst and adsorbent [8], in addition to being a drug delivery carrier [9, 10]. This entire application spectrum requires tailoring of the different properties of MpAl, such as particle size and morphology, which can be done by using planned synthetic routes [11]. The narrow pore size distribution, higher surface areas and abundance of surface hydroxyl groups of MpAl is responsible for its extraordinary properties, compared with conventional aluminas [12]. Various factors, such as starting materials (alkoxides, metal salts etc.), surfactants as a structure directing agent, reaction parameters (pH, temperature, solvent, co-solvent etc.) influence the formation of porous structures and dictate the pore size, its distribution and ordering in MpAl [13]. To date, diverse methods have been reported for the synthesis of MpAl, such as spray pyrolysis [14], which experience some major limitations such as (i) larger grain size because of uncontrollable spray droplet size, (ii) wastage of solution and (iii) low deposition rate [15]. Hydrothermal MpAl synthesis using a teflon-lined stainless steel autoclave [16, 17], may be tedious because of control of intermediate parameters such as temperature, pH and the concentration of reacting solutions, and the requirement of a pressurised instrument such as a teflon-lined stainless steel autoclave. Researchers have also reported a DC plasma spray torch for the synthesis of MpAl, where traces of impurities such as iron and carbon were observed because of the plasma reactor [18]. Other methods such as microemulsion templating are also found in the literature, but they are more time-consuming [19].

The simplicity of the sol–gel technique is a blessing for inorganic material synthesis because of its versatility and excellent control over a product's properties; in addition, the process allows relatively facile tailoring of the morphology of mixed oxides to the desired applications [20]. It is not only a suitable approach for laboratory-scale preparations [1] but is also a cost-effective method, yielding amorphous and poorly crystalline materials with high surface area and small pore sizes [21].

To date, in most of the reported papers for the synthesis of MpAl, the researchers have used either aluminium alkoxide or sodium aluminate as a precursor. In the present investigation, we propose the use of aluminium chloride as the precursor and cetyl trimethyl ammonium bromide (CTAB) as a template for the mesoporous structure, as the combination of aluminium chloride hexahydrate and CTAB has not been explored yet. Apart from the use of the novel precursor, the study further explores the use of ethanol for varying the pore size of the synthesised mesoporous nanoparticles. The present investigation deals with the sol–gel synthesis of MpAl by hydrolysis of the parent precursor of aluminium salt (aluminium chloride hexahydrate) followed by polycondensation in a surfactant solution. After a specific ageing time it forms a mesostructure when calcined at 700°C for 6 h. Urea was used as a support in the hydrolysis medium and 28–30% of the ammonia solution was used as the precipitating agent. The uncontrolled phase separation between the inorganic and the organic components was prevented by precisely controlling the reaction conditions which resulted in a higher degree of cross-linking between the precursor molecules.

## 2. Material and methods

**2.1. Synthesis of MpAl:** The technique of MpAl synthesis (stirred sample) involves refluxing a solution of 1.4 g of CTAB surfactant into 23 ml of ethanol on a magnetic stirrer and allowing it to reach the reaction temperature up to 70°C. To this solution, a sonicated solution of 2.6 g of aluminium chloride and 0.7 g of urea in 20 ml water was added in a dropwise manner. After 30 min of reaction, 6 ml of 28–30% ammonia solution was added dropwise. The reaction was continued further for 2 h at 70°C. After the selected ageing time of about 3–6 h, the solvent was removed by heating at 100°C for 5–7 h, the resulting precipitate was calcined in the flowing air of the furnace by heating at 1°C/min up to 700°C and then kept at the same temperature for 6 h. For the unstirred sample, the same procedure was adopted except for the step of stirring.

**2.2. Characterisation of synthesised MpAl:** The synthesised MpAl was characterised using Fourier transform infrared spectroscopy (FTIR) for confirming the formation of MpAl supported by an

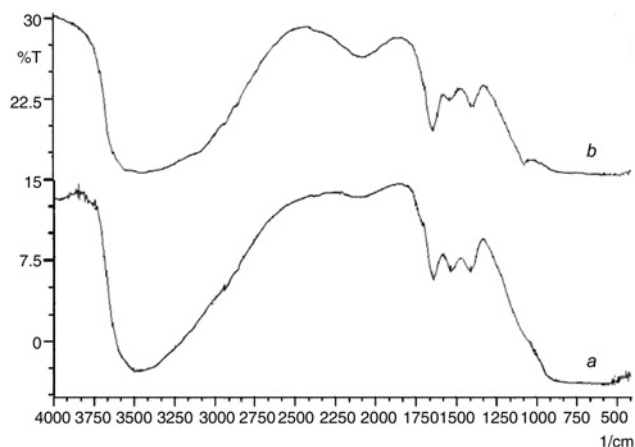


**Figure 1** FTIR spectra of synthesised MpAl  
*a* Stirred sample; *b* Unstirred sample

energy dispersive X-ray spectroscopy (EDX) study for confirming the presence of alumina. The crystallinity of synthesised MpAl was studied using X-ray diffraction (XRD) analysis. The study of surface morphology was performed by using field emission scanning electron microscopy (FESEM). Brunauer-Emmett-Teller analysis was conducted to study the pore size and the size distribution of synthesised MpAl. Particle size and surface charge were determined by using Malvern Zeta Sizer.

The FTIR (FTIR – IR-Affinity 1700, Shimadzu) spectrum was used to monitor the MpAl synthesised with and without stirring (Fig. 1), which gave primary confirmation of MpAl formation. It revealed an absorption band at 3450–3500  $\text{cm}^{-1}$  because of the presence of an OH group in formed MpAl. The template molecules comprised an alkyl chain and their characteristic peaks were observed at the 2855 and 2925  $\text{cm}^{-1}$  range. The principal groups were carboxylic acid salts, which appeared in the 1650–1550  $\text{cm}^{-1}$  range (asymmetric  $\text{COO}^-$  stretching) and 1440–1335  $\text{cm}^{-1}$

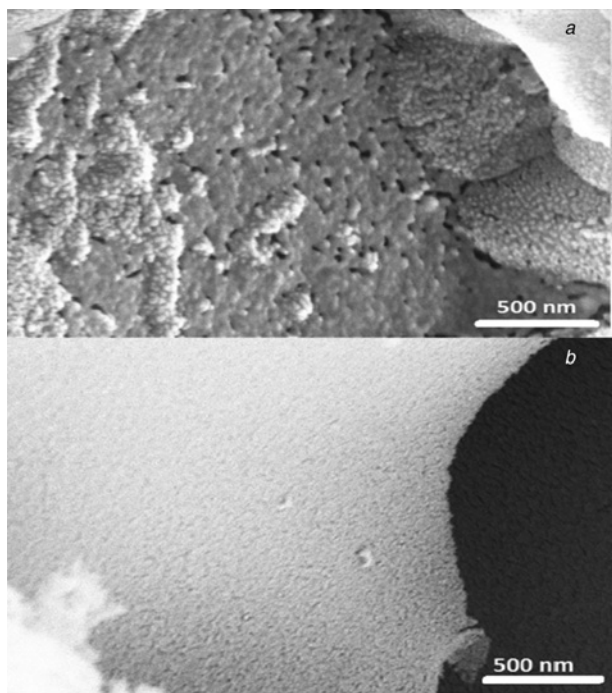


**Figure 2** FESEM images of synthesised MpAl  
*a* Stirred samples  
*b* Unstirred samples

range (symmetric  $\text{COO}^-$  stretching, usually two or three peaks) [22]. The results of the FTIR analysis confirmed the formation of MpAl by using the alumina precursor.

The surface morphology of the MpAl was studied using a field emission electron microscope (Hitachi S-4800, America) of synthesised MpAl. It revealed the granular structure of the stirred samples with random pore distribution (Fig. 2*a*) whereas spongy and uniform pore distribution of the unstirred sample was confirmed using FESEM (Fig. 2*b*). The FESEM image of the hierarchical porous alumina shows disordered large pores. From the high-magnification FESEM image (Fig. 2*b*), the mesostructure could be observed clearly on the frameworks with large pores, suggesting that the hierarchical porous materials are mainly composed of mesopores, hence these samples were subjected to further analysis.

Elemental analysis of synthesised MpAl was conducted for confirming the presence of alumina, and for the simultaneous determination of impurities, if any, in situ EDX analysis was conducted. The spectra (Fig. 3) indicated the presence of  $\text{Al}_2\text{O}_3$  with an insignificant amount of impurities after calcination. The EDX spectrum revealed the presence of 67.57% O (oxygen) and 32.46% Al depending on its molecular formula. The absence of impurities shows that the proposed method using the novel precursor helps in the synthesis of MpAl with high purity.

Preliminary powdered X-ray (D8 Advanced X-ray Diffractometer Bruker, Germany) diffraction data showed the formation of  $\gamma\text{-Al}_2\text{O}_3$  at a calcination temperature of 700°C. It was in compliance with the published literature [23, 24]. The XRD pattern of the sample corresponds to the MpAl nanoparticles and demonstrated the crystalline nature of MpAl from 20° to 80° (Fig. 4). Three broad, low intensity peaks that are typically attributed to gamma alumina were observed at 32°, 46° and 67°.

The nitrogen adsorption–desorption isotherms and the corresponding pore-size distribution curves of the as-synthesised alumina powders are shown in Figs. 5*a* and *b*, respectively. The typical curve with a hysteresis loop which can be attributed to cylindrical mesoporous channels present in MpAl can be observed. The pore size distribution of MpAl (Fig. 5*b*), derived from the adsorption branch of the isotherm by using the Barrett-Joyner-Halenda model is centred at 4.5 nm.

The nitrogen sorption isotherms and corresponding pore size distribution curves of the synthesised MpAl are shown in Fig. 5. A strong uptake of  $\text{N}_2$  as a result of capillary condensation is observed in a relative pressure ( $p/p_0$ ) of 0.02 and reaches a turning point at 0.096, which suggests that the final materials belong to the mesoporous family, with pore sizes close to 4.5 nm.

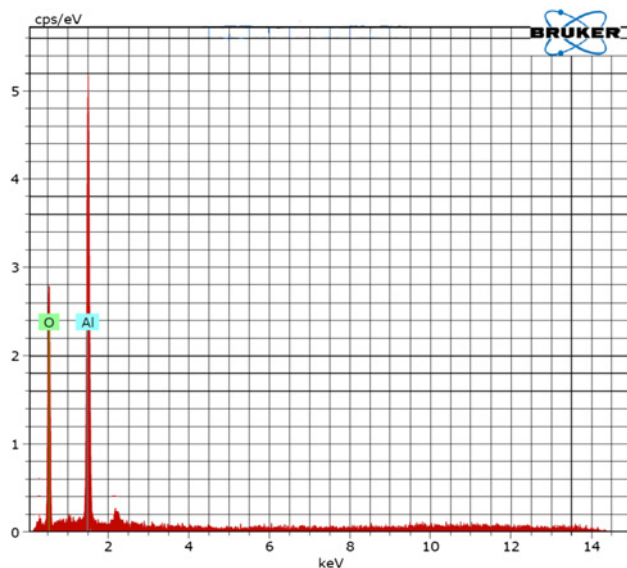


**Figure 3** EDX spectrum of MpAl nanoparticles

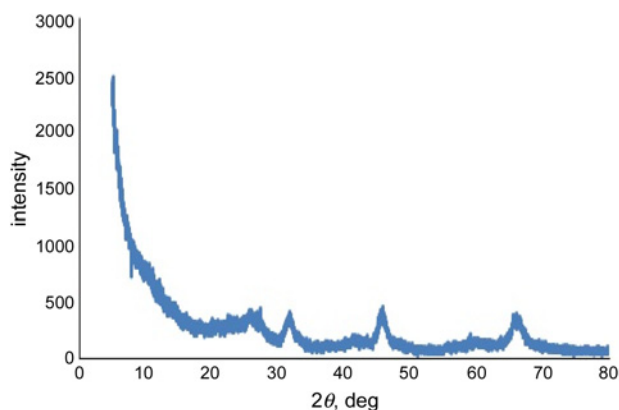


Figure 4 XRD pattern for MpAl nanoparticles

Malvern Zeta Sizer was used for determining the surface charge and the potential. There is less in the literature about the determination of the point of zero charge (PZC); in the present investigation, PZC was estimated using the Malvern Zeta Analyser (ZS90) for MpAl. In the case of oxides such as alumina, the potential-determining role of  $H^+$  and  $OH^-$  charge transfer across the alumina–water interface are determined by the equilibrium of  $H^+$  and  $OH^-$  with  $Al^{+++}$  and  $O^{2-}$  in the lattice, as reported elsewhere [25].

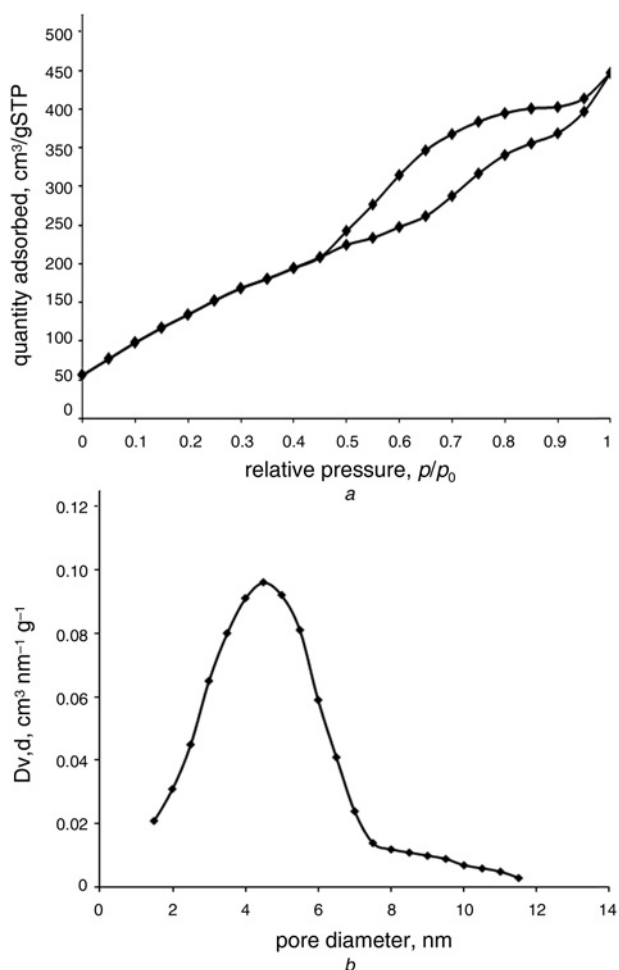


Figure 5 Nitrogen sorption isotherm and corresponding pore size distribution of MpAl nanoparticles  
a Nitrogen sorption isotherm  
b Pore size distribution

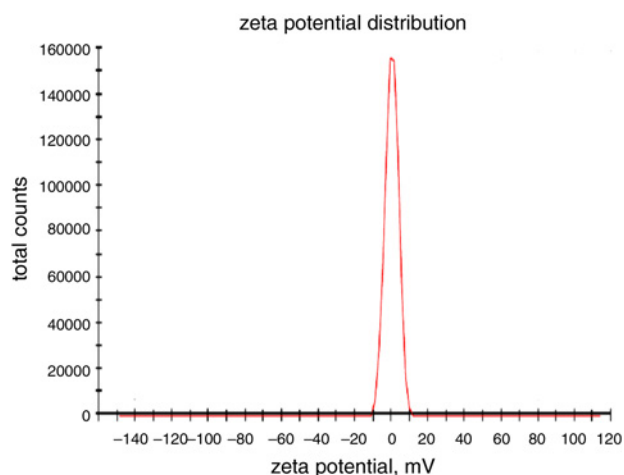


Figure 6 Zeta potential of MpAl nanoparticles

In the present study, no electrophoretic mobility was observed in the presence of the applied electric field, which can be correlated with the absence of surface charge on MpAl nanoparticles (Fig. 6).

**3. Conclusion:** MpAl nanoparticles with uniform surface morphology can be synthesised using this simple route by means of CTAB as a surfactant template. This route has been found to be reproducible and avoids the need for strict control of the hydrolysis conditions. Stirring can enhance particle aggregation as evident from FESEM. Unstirred synthesis yielded better results with almost uniform pore distribution. In the future, synthesised MpAl could be employed as a platform for various applications such as chemical reaction, catalysis, semiconductors, ceramics, nanocomposites and electrochromic displays. Moreover, the surface properties of MpAl, particularly the modification of the surface hydroxyl group by using a suitable coupling agent may prove useful.

**4. Acknowledgment:** The authors thank the Principal and Management of HRPIPER for providing all the necessary requirements for achieving the research objectives.

## 5 References

- [1] Fadeel B., Garcia-Bennett A.E.: 'Better safe than sorry: understanding the toxicological properties of inorganic nanoparticles manufactured for biomedical applications', *Adv. Drug Deliv. Rev.*, 2010, **62**, (3), pp. 362–374
- [2] Liu C., Liu Y., Ma Q., He H.: 'Mesoporous transition alumina with uniform pore structure synthesized by alumisol spray pyrolysis', *Chem. Eng. J.*, 2010, **163**, (1–2), pp. 133–142
- [3] Vaudry F., Kohdabandeh S., Davis M.E.: 'Synthesis of pure aluminas mesoporous materials', *Chem. Mater.*, 1996, **8**, p. 1451
- [4] Yada M., Machida M., Kijima T.: 'Synthesis and deorganization of an aluminium-based dodecyl sulfate mesophase with hexagonal structure', *Chem. Commun.*, 1996, **6**, p. 769
- [5] Bagshaw S.A., Pinnavaia T.J.: 'Mesoporous alumina molecular sieves', *Angew. Chem. Int. Ed. Eng.*, 1996, **35**, (10), pp. 1102–1105
- [6] Kim C., Kim Y., Kim P., Yi J.: 'Synthesis of mesoporous alumina by using a cost-effective template', *Korean J. Chem. Eng.*, 2003, **20**, (6), pp. 1142–1144
- [7] Nazari A., Riahi S., Riahi S., Shamekhi S.F., Khademno A.: 'Influence of  $Al_2O_3$  nanoparticles on the compressive strength and workability of blended concrete', *J. Am. Sci.*, 2010, **6**, (5), pp. 6–9
- [8] Cejka J.: 'Organised mesoporous alumina: synthesis, structure and potential in catalysis', *Appl. Catal. A-Gen.*, 2003, **254**, (12), pp. 327–338
- [9] Das S.K., Kapoor S., Yamada H., Bhattacharyya A.J.: 'Effects of surface acidity and pore size of mesoporous alumina on degree of loading and controlled release of ibuprofen', *Micropor. Mesopor. Mater.*, 2009, **118**, pp. 267–272

- [10] Kapoor S., Hegde R., Bhattacharyya A.J.: 'Influence of surface chemistry of mesoporous alumina with wide pore distribution on controlled drug release', *J. Control. Release*, 2009, **140**, pp. 34–39
- [11] Saber O.: 'Novel self assembly behavior for  $\gamma$ -alumina nanoparticles', *Particuolog.*, 2012, **10**, (6), pp. 744–750
- [12] Ramli Z., Chandren S.: 'Effect of templates on the synthesis of organised mesoporous alumina', *Malays. J. Anal. Sci.*, 2007, **11**, (1), pp. 110–116
- [13] Naik B., Ghosh N.N.: 'A review on chemical methodologies for preparation of mesoporous silica and alumina based materials', *Recent Patents Nanotechnol.*, 2009, **3**, pp. 213–224
- [14] Kim J.H., Jung K.Y., Park K.Y.: 'Effect of urea,  $\text{NH}_4\text{OH}$  and DCCA on texture properties of alumina prepared by ultrasonic spray pyrolysis', *J. Ind. Eng. Chem.*, 2012, **18**, (1), pp. 344–348
- [15] Jeyaprakash B.G., Ashok kumar R., Kesavan K., Amalarani A.: 'Structural and optical characterization of spray deposited SnS thin film', *J. Am. Sci.*, 2012, **6**, (3), pp. 22–26
- [16] Yue M.B., Xue T., Jiao W.Q., Wang Y.M., He M.Y.: 'CTAB-directed synthesis of mesoporous  $\gamma$ -alumina promoted by hydroxyl carboxylate; the interplay of tartrate and CTAB', *Solid State Sci.*, 2011, **13**, (2), pp. 409–416
- [17] Patra A.K., Dutta A., Bhaumik A.: 'Self assembled  $\text{Al}_2\text{O}_3$  spherical nanoparticles and their efficiency for the removal of arsenic from water', *J. Hazard. Mater.*, 2012, **201**, pp. 170–177
- [18] Suresh K., Selvarajan V., Vijay M.: 'Synthesis of nanophase alumina, and spheroidization of alumina particles, and phase transition studies through DC thermal plasma processing', *Vacuum*, 2008, **82**, (8), pp. 814–820
- [19] Zhang X., Zhanga F., Chan K.Y.: 'The synthesis of large mesopores alumina by microemulsion templating, their characterization and properties as catalyst support', *Mater. Lett.*, 2004, **58**, pp. 2872–2877
- [20] Ward D.A., Ko E.I.: 'Preparing catalytic materials by the sol–gel method', *Ind. Eng. Chem. Res.*, 1996, **34**, p. 421
- [21] Ecsedi Z., Lazau I., Pacurariu C.: 'Synthesis of mesoporous alumina using polyvinyl alcohol template as porosity control additive', *Process. Appl. Ceramics*, 2007, **1**, (1–2), p. 5
- [22] Kim Y., Kim C., Kim P., Yi J.: 'Effect of preparation conditions on the phase transformation of mesoporous alumina', *J. Non-Cryst. Solids*, 2005, **351**, (6–7), pp. 550–556
- [23] Smith S.J., Amin S., Woodfield B.F., Goates J.B., Campbell B.J.: 'The phase progression of  $\gamma$ - $\text{Al}_2\text{O}_3$  nanoparticles synthesized in solvent deficient environment', *Inorg. Chem.*, 2013, **52**, pp. 4411–4423
- [24] Wu Q.: 'Synthesis of ordered mesoporous alumina with large pore sizes and hierarchical structure', *Micropor. Mesopor. Mater.*, 2011, **143**, (2–3), pp. 406–412
- [25] Yopps J.A., Fuerstenau D.W.: 'The zero point of charge of alpha-alumina', *J. Coll. Sci.*, 1964, **19**, p. 61